Optics Communications 283 (2010) 2961–2966

Contents lists available at ScienceDirect

Optics Communications

journal homepage: www.elsevier.com/locate/optcom

Characteristics of light emission from surface plasmons based on rectangular silver gratings

Seung Ho Choi [a], Sung June Kim [a,b], Kyung Min Byun [c,*]

[a] Interdisciplinary Program of Bioengineering, Seoul National University, Seoul, 152-742, Republic of Korea
[b] School of Electrical Engineering and Computer Science, Seoul National University, Seoul, 151-742, Republic of Korea
[c] Department of Biomedical Engineering, Kyung Hee University, Yongin, 446-701, Republic of Korea

ARTICLE INFO

Article history:
Received 20 November 2009
Received in revised form 20 March 2010
Accepted 22 March 2010

Keywords:
Surface plasmons
Silver gratings
Transmission
Silver oxidation
Biosensor

ABSTRACT

We investigated the characteristics of transmitted light from propagating surface plasmons based on rectangular silver gratings. The results calculated by rigorous coupled-wave analysis presented that silver diffraction gratings can produce significant transmittance and conversion efficiency, comparable to the case of dielectric gratings. Especially, silver gratings optimized at a wide range of grating thickness and period may lead to an improved diffraction efficiency larger than 64%. Moreover, the effect of silver oxide layer on the transmittance was examined and a bimetallic structure with a thin gold coating was introduced to prevent an oxidation of silver substrates. As a practical sensor application, silver grating-based surface plasmon resonance (SPR) configuration showed an enhanced sensitivity associated with an increase of surface reaction area and strong excitations of local plasmon fields, outperforming a conventional thin-film-based SPR structure.

1. Introduction

The phenomenon of surface plasmon resonance (SPR) has been used in a variety of applications such as biosensing, microscopy, optical waveguiding, lithography, and light sources [1]. Surface plasmons (SPs) are collective oscillations of free electron gas density. Especially, if the momentum of incident light matches that of the SPs, the light energy is absorbed and SP waves are resonantly excited [2].

Recently, conversion of SPs into a radiation mode has been investigated to overcome the limitations of a conventional SPR structure based on the Kretschmann configuration [3,4]. For example, as detection range of SPR biosensor is intrinsically confined to the penetration depth with a dimension of several hundred nanometers, a thin-film-based SPR system has difficulties in sensing massive and bulky target analytes. On the other hand, radiative emission of a propagating SP by a diffraction grating can allow one to measure transmission characteristics of thick target samples such as in cell analysis. In other words, diffraction gratings enable the transmitted light to sense the target's status variation by means of transmittance or scattering, e.g., due to morphological changes of thick samples, while the surface-limited depth of SPR detection does not change significantly. Moreover, it enables integration of optical devices, e.g., a light modulator and polarization filter, into miniaturized photonic circuits.

Since the first introduction of dielectric diffraction gratings for an efficient transformation of SP waves into transmission modes, we have studied the profile effect of a dielectric grating on the transmittance [5]. From our previous results, we showed that dielectric gratings on a silver film led to a significant diffraction efficiency and dielectric gratings with a pyramid profile had a higher transmittance than the other profiles, resulting in a peak value of 77% at the optimum grating structure. Although the use of dielectric gratings might be suitable for an excitation of radiation modes, metallic gratings are also plausible to outcouple surface plasmons [6].

Thus, in this study, a transmission-type SPR configuration with silver gratings built on a silver film is investigated for effective conversion of SP waves into a radiative light. The effect of silver gratings on the transmission characteristics has been analyzed theoretically using rigorous coupled-wave analysis (RCWA) [7]. First, transmission characteristics for silver gratings are presented with the aim to maximize the transmittance of propagating SP waves. An interesting possibility of a formation of silver oxide layer (Ag_2O) on a silver substrate is then described because silver coatings are known to be highly susceptible to oxidation. Since an oxide layer may significantly affect the resonance condition of SP waves and diffraction efficiency, the influence of Ag_2O layer on the transmittance should be estimated. Also, an alternative structure of bimetallic Au/Ag surface, where a thin gold film is added to protect a silver layer from oxidation is explored.

Subsequently, after further design optimization for a rectangular silver grating, its actual application as an optical biosensor is examined in comparison with a conventional SPR biosensor. Contrary

* Corresponding author.
E-mail address: kmbyun@khu.ac.kr (K.M. Byun).

0030-4018/$ – see front matter © 2010 Elsevier B.V. All rights reserved.
doi:10.1016/j.optcom.2010.03.054

to our previous application of a silver grating for detection of refractive index change occurring at overall ambience [6], practically important sensor scheme that measures biomolecular interactions adsorbed on a sensor substrate is displayed in this study. Note that the presence of silver grating may improve the sensor performance because sensitivity can be enhanced by an increase of surface reaction area which mediates additional interactions between excited plasmons and local binding events and by localized surface plasmon (LSP) excitations with strongly enhanced field intensity [8]. From the results of this study, we intend to show a potential for diversifying the use of radiative SP fields in a sensitive detection of biomolecular interactions and various optical devices.

2. Numerical model

Silver grating-mediated transmission-type SPR configuration was numerically calculated using RCWA which has been successful in describing experiments with dielectric or metallic nanostructures [9,10]. When a light source is assumed to be a unit-amplitude and monochromatic plane wave with a wavelength λ and an incidence angle θ with the z-axis, a magnetic field inside a metallic grating region is determined by solving the wave equation [11],

$$\nabla^2 H + \frac{\nabla \varepsilon}{\varepsilon} \times \nabla \times H + k^2 \varepsilon(x,z) H = 0 \quad (1)$$

where H is the magnetic field and k ($=2\pi/\lambda$) is the wave number in the free space.

For TM-polarized light, Eq. (1) can be converted into,

$$\nabla^2 H - \left(\frac{\nabla \varepsilon}{\varepsilon} \cdot \nabla\right) H + k^2 \varepsilon(x,z) H = 0. \quad (2)$$

$\varepsilon(x,z)$ is the complex dielectric function of a metallic grating and is written as a Fourier series expansion of

$$\varepsilon(x,z) = \varepsilon(x+\Lambda,z) = \sum_a \varepsilon_m(z) \exp(jaK_G x), \quad (3)$$

where Λ is the grating period, ε_m is the Fourier component of the grating's dielectric function, and K_G ($=2\pi/\Lambda$) is the grating vector, respectively. In the computation, RCWA is expressed as an infinite set of coupled-wave equations where the magnetic field is expanded in terms of spatial harmonic components with variable amplitudes in the z-direction. The spatial harmonic amplitudes are then solved for the coefficient matrix based on eigenvalues and eigenvectors of the differential equation. Although the whole coefficient matrix is an infinite one, calculation results can be obtained to an arbitrary level of accuracy of a truncated matrix [12]. The continuity of the tangential components of electromagnetic fields at the boundaries between media can be employed to determine the unknown coefficients as well. Finally, each space-harmonic component inside a metallic grating is phase-matched to individual diffraction order. Details of RCWA can be found elsewhere [13]. Note that since the field varies more rapidly in short distances of a grating with a size smaller than a wavelength λ, more space-harmonic orders are required to achieve the convergence and to improve the accuracy in calculations. For the simulation presented in this study, 30 spatial harmonics have been considered, unless otherwise noted.

Prior to an in-depth analysis on the proposed SPR structure, it might be necessary to describe the effect of substrate material on an excitation of SP waves. Among various noble metals, gold and silver have been generally utilized to excite surface plasmons due to their low damping properties. However, most of the earlier studies on grating-coupled transmission-type SPR configurations have employed a silver layer because a transmitted light by a silver substrate shows better diffraction characteristics. Fig. 1 presents the calculated transmittance of SP waves

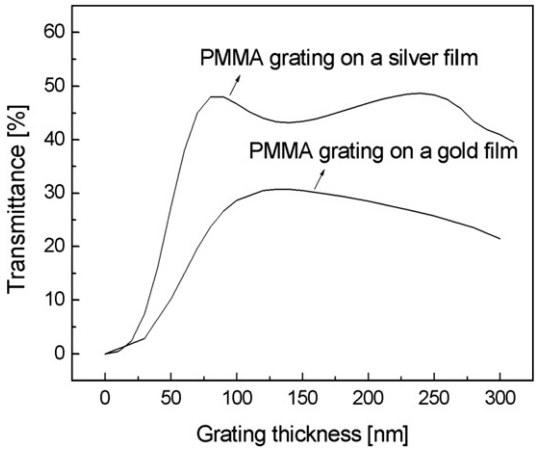

Fig. 1. Transmission characteristics of the first-order beams diffracted by PMMA gratings built on gold and silver films. Rectangular PMMA gratings have a period of Λ = 650 nm and a fill factor of f = 0.5 and a thickness of thin metal film on a BK7 prism substrate is fixed at 40 nm. TM-polarized monochromatic plane wave with λ = 633 nm is incident on a prism and the diffracted light transmits into an air environment. The optical constants (n, k) of a BK7 glass, silver and gold films, and PMMA gratings were determined as (1.515, 0), (0.059, 4.243), (0.18, 3.0), and (1.50, 0) at λ = 633 nm.

by polymethyl methacrylate (PMMA) gratings with a period Λ = 650 nm and a fill factor f = 0.5. When a TM-polarized light at λ = 633 nm is incident through a BK7 prism substrate, resonantly excited SP waves propagate along the metal surface and a diffracted light by PMMA gratings on a silver film achieves a maximum transmittance of 48%. On the other hand, when a gold film is applied, the peak efficiency obtained is 30% at a grating thickness of 130 nm and a low transmittance <20% appears at a thick grating with a thickness larger than 300 nm. This contrast in diffraction efficiency is attributed to the fact that SP waves along the silver film are less attenuated and thus, silver shows a longer propagation length and a deeper penetration depth into dielectric medium than SP waves supported by a gold film [14]. Consequently, we considered silver as a substrate material throughout this work.

A schematic diagram of a silver grating-mediated SPR configuration is drawn in Fig. 2. One-dimensional arrays of infinitely long silver gratings with a period Λ are regularly distributed on a metal film that supports SP waves. A 40-nm thick silver film is deposited on a BK7 prism substrate, on which polarized light at λ = 633 nm is incident. A fill factor f, a volume concentration of a grating per period is fixed at

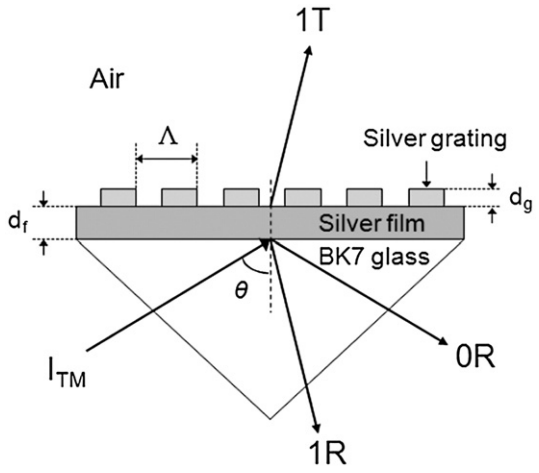

Fig. 2. Schematic diagram of a transmission-type SPR configuration with rectangular silver gratings. A 40 nm thick silver film is deposited on a BK7 prism substrate. Silver gratings with a period Λ and a thickness d_g have a constant fill factor of f = 0.5. TM-polarized light is incident through the prism substrate at a wavelength of λ = 633 nm and the first-order diffraction beam radiates into the air environment.

$f=0.5$ to exclude the effect of grating volume on the diffraction efficiency. The optical constants (n, k) of BK7 glass prism, silver film, and silver oxide were determined as (1.515, 0), (0.059, 4.243), and (2.50, 0.11), respectively, at $\lambda=633$ nm [3,15]. Reflectance (0R) and transmittance (1 T) curves were obtained from RCWA calculations as the angle of light incidence is scanned with an angular resolution of 0.01°. Under the condition of 30 diffraction orders, it was found that maximum error deviations of both resonance angle and diffraction efficiency were as low as 1%.

By solving Maxwell equations, the dispersion relation of the resonant SP waves can be obtained and is given by

$$k_{SPR} = k_0\sqrt{\varepsilon_p}\sin\theta_{SPR}, \tag{4}$$

where k_{SPR} and k_0 are the wave vectors of the SP and the incident light. ε_p is the dielectric function of a prism substrate and θ_{SPR} is the incidence angle at resonance [2]. Propagating surface plasmons are transformed into a radiation mode when the following condition is satisfied;

$$k_q = k_{SPR} - qK, \quad q = 0, \pm1, \pm2, \ldots \tag{5}$$

where k_q is the wave vector of the q-th diffracted light and K ($=2\pi/\Lambda$) is the grating vector. Especially, a limited range of grating periods almost equal to or less than the wavelength of an incidence is chosen in RCWA calculation, so that only the low diffraction orders can be emitted into the air.

3. Results and discussion

Fig. 3 shows the characteristics of transmittance, resonance angle, and conversion efficiency (CE) of a rectangular silver grating as a function of the grating thickness. Silver gratings have a period of $\Lambda=600$ nm and a fill factor of $f=0.5$. The grating thickness with maximum transmittance was determined to be $d_g=23$ nm with $1T_{MAX}=53.3\%$, which is comparable to the results for dielectric diffraction gratings in Fig. 1. At the range of $d_g>50$ nm, however, significant attenuation of radiation modes was observed due to the high absorption coefficient of silver, so that the transmittance was decreased to less than 20%. Also, when the grating thickness varies, the resonance angle increases slightly. The peak transmittance was obtained at an incidence angle of 43.32°. Especially, an abrupt reduction of the first-order transmittance was found at $d_g=20$ nm, which is associated with geometry-dependent excitation of localized plasmon. The details will be described in subsequent discussions.

What is as important as transmittance is CE, which is introduced to estimate the diffraction performance of rectangular silver gratings. In principle, incident beam is highly absorbed and converted into SP waves at the resonance condition. The plasmons propagating along the metal surface are partially absorbed into the metal film and partially diffracted into airspace by silver gratings. In order to quantify this, the CE is defined as the ratio of the radiation intensity of the first-order diffraction to the adsorbed incidence beam intensity into SP waves, i.e., CE = first-order transmittance/(1 − zeroth-order reflectance). As a result, a larger CE approximately equal to 1 is required to achieve a higher transmittance, though it is evidently difficult to obtain such a high CE due to various plasmonic damping effects of silver substrates. The peak CE was obtained to be 70.6% at $d_g=32$ nm and an incidence angle of 43.63°. However, it is important to notice that an increase of metallic grating thickness induces a resonance dip to become broad and shallow substantially, often for thick gratings of $d_g\geq30$ nm in an air medium [16]. In other words, regardless of the transmittance performance, CE value can be improved even for thick silver gratings due to a shallow reflectance curve. Since high CE values obtained from a shallow reflectance would not be useful practically,

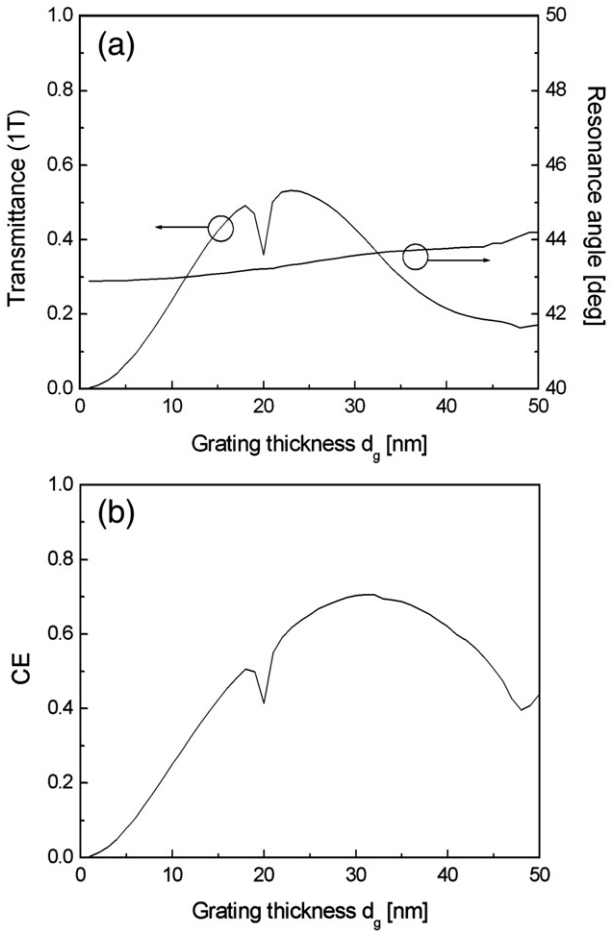

Fig. 3. (a) Transmittance, resonance angle, and (b) CE characteristics of rectangular silver gratings as a function of the grating thickness.

silver gratings with an increasing CE at $d_g>45$ nm should be left out of consideration.

Also, of interest is the influence of silver oxide layer, which can be formed by reactive sputtering of pure silver in an oxygen-containing argon atmosphere or by thermal or e-beam evaporation of pure silver followed by oxidation in an oxygen plasma [17]. When uniform Ag_2O layers are applied to the surface boundaries of silver substrates, an oxidation of a pure silver film into Ag_2O is accompanied by an increment in thickness. It has been found that the growth of the Ag_2O layer occurs at the expense of the underlying Ag film and its thickness is close to 1.5 times that of the converted Ag layer [15]. Fig. 4 shows the calculated change in diffraction efficiency when Ag_2O is formed on silver substrates with the rectangle grating of $d_g=23$ nm and $\Lambda=600$ nm. As the thickness of silver oxide increases, the diffracted light may experience a destructive interaction with Ag_2O layers due to the dephasing of the fundamental first-order diffraction mode. This in turn can induce a considerable degradation of diffraction efficiency.

In order to overcome the drawbacks of Ag_2O formation, a bimetallic surface where a thin gold layer is coated over the silver substrate to protect it from oxidation is proposed as an alternative transmission-type SPR structure. In Fig. 5, the first-order diffraction efficiency calculated for rectangular silver gratings with $d_g=23$ nm and $\Lambda=600$ nm is shown. When a thickness of a gold film with a uniform coverage is increased, the transmittance decreases monotonically. This is because an attachment of gold layer with a larger attenuation than silver may cause the radiative modes to be generated ineffectively. Therefore, it is important to realize an extremely thin gold layer, so that a high transmittance obtained from silver gratings would not be decayed by an additional thin gold layer. In terms of

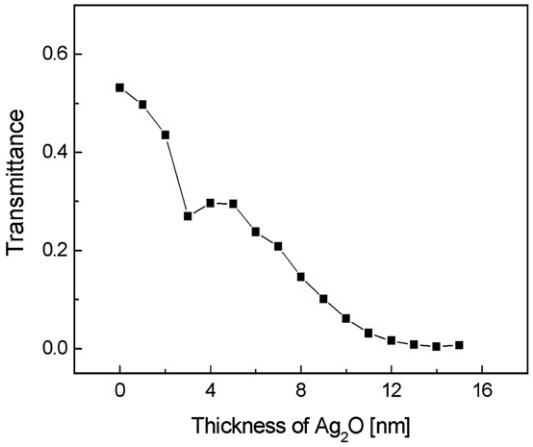

Fig. 4. Calculated transmittance for silver gratings at $d_g = 23$ nm and $\Lambda = 600$ nm when the thickness of Ag_2O layer increases.

practical implementation of a bimetallic substrate, though difficulties in fabrication may increase, ultrathin gold films can be obtained by sputtering a gold target by means of argon ion and oxygen ion beams [18].

So far, the influences of silver gratings on the transmission characteristics have been explored when the grating period is fixed at $\Lambda = 600$ nm. As a next step, the first-order diffraction efficiency of a rectangular silver grating was additionally calculated as a function of grating period and thickness to maximize the transmittance. In Fig. 6(a), it was found that a large transmittance over 50% was achieved at a wide range of Λ and d_g, which represents the reliability in both performance and fabrication. The peak efficiency was obtained to be as high as 64.1% at $d_g = 12$ nm and $\Lambda = 330$ nm and this transmittance is comparable or even larger in comparison with the case of dielectric diffraction gratings. However, it should be mentioned that a significant reduction of transmittance was found as denoted by solid and dotted lines.

A reduction of the first-order transmittance along the solid line is associated with an excitation of LSP resonance. Especially, since this absorption occurs only for the grating period (Λ)/thickness (d_g) ratio of 30, it suggests geometry-dependent excitations of LSP modes. An extra absorption of metallic structures at particular wavelength and geometry is a well known phenomenon combined with localized plasmons [19,20]. While the results are not shown, it was confirmed that the vertical absorption band in Fig. 6(a) changes with the fill factor of rectangular silver gratings. More in-depth analyses on the geometry-dependent LSP resonance for various grating profiles and its influence on the transmission characteristics will be demonstrated

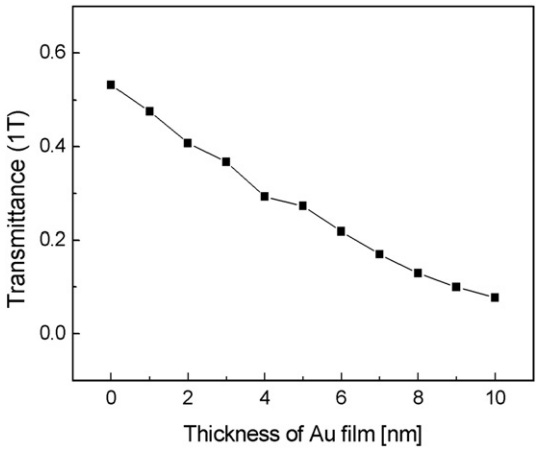

Fig. 5. Calculated transmittance for silver gratings at $d_g = 23$ nm and $\Lambda = 600$ nm when the thickness of a thin gold film coated on a silver substrate increases.

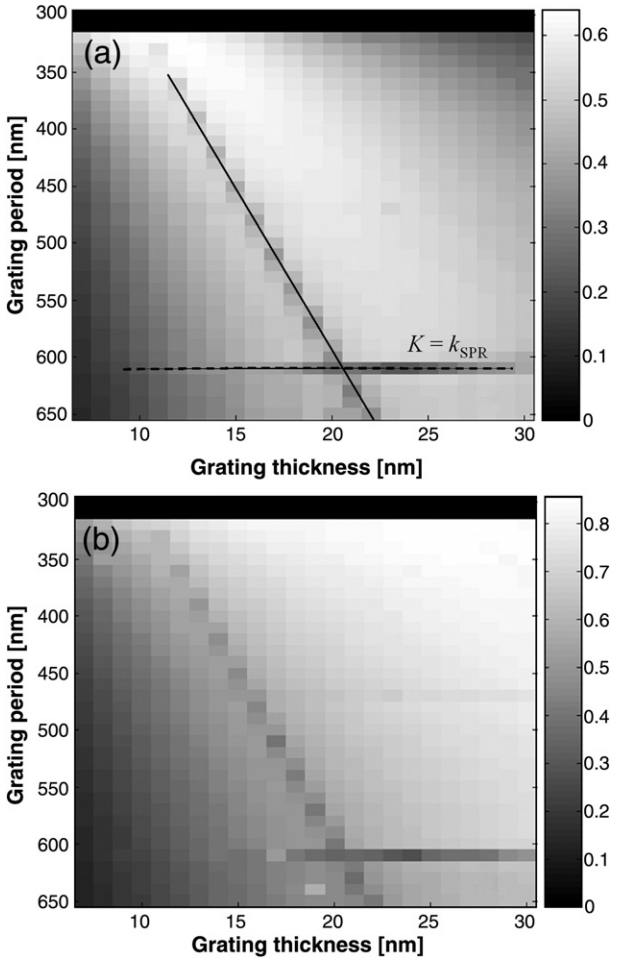

Fig. 6. (a) Transmittance and (b) CE of the first-order diffraction beam for the silver grating when the grating period varies from 300 to 650 nm and the thickness from 7 to 30 nm. The solid and dotted lines indicate the effects of geometry-dependent LSP resonance and plasmon radiation damping, respectively.

in our subsequent studies. Another interesting topic connected with LSP excitations is the effect of a direct contact of silver gratings to a thin silver film, because most of earlier studies on LSP resonance are based on the metallic subwavelength structure supported by a dielectric substrate. To reveal a possible assertion that a direct attachment of silver gratings to a metallic substrate may dampen localized plasmons, we calculated near-field characteristics in the vicinity of silver substrates using finite-difference time-domain (FDTD) methods. One of the rectangular silver gratings on the vertical solid line in Fig. 6(a) was chosen as $\Lambda = 540$ nm and $d_g = 18$ nm. The minimum grid size for the FDTD calculation was 1.0 nm and the field distribution E_Z was obtained at an incidence of 43.16°, which can provide the peak transmittance of 38%.

FDTD results in Fig. 7 exhibit typical features of LSPs excited by metallic subwavelength structures. Locally enhanced fields are distributed at very short distance from the surface in the vicinity of grating vertices. Four different peaks associated with each corner of the silver gratings are formed by an interaction between propagating surface plasmons and silver gratings. Since the decay length of an LSP mode is shorter than the interpeak distance, the multiple peaks of each corner should be regarded as an individual LSP resonance. On the assumption that the incident beam is of unit amplitude, maximum field was obtained as $E_Z = 40.0$ at the upper two vertices of the silver gratings. At the lower two vertices, however, amplitude of enhanced fields is much smaller than that of the upper ones and has a peak value of $E_Z = 15.7$. FDTD results display that the direct contact may induce a

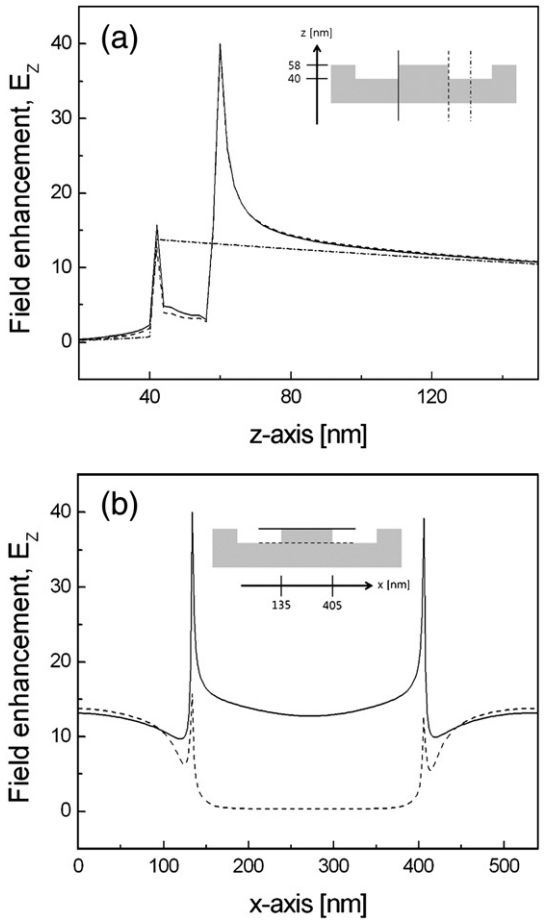

Fig. 7. (a) Vertical and (b) horizontal field amplitude distributions of E_Z around the silver substrate for rectangular silver gratings of $f=0.5$, $d_g=18$ nm, and $\Lambda=540$ nm.

damping of localized plasmons and therefore, significant degeneration of localized plasmons is obtained.

Another low transmittance region indicated by the dotted line can be explained analytically using the effect of radiation damping [5]. When a diffracted light of 2R propagates along the trace that exactly overlaps the incidence, the incident beam can be highly degenerated through a destructive coupling between the incidence and the diffracted light. This phenomenon may occur when the grating vector K equals the wave vector k_{SPR} of the SP waves and can be expressed as

$$K = k_{SPR} = k_0\sqrt{\varepsilon_p}\sin\theta_{SPR}. \tag{6}$$

Fig. 6 clearly show that the line $K=k_{SPR}$ obtained from Eq. (6) matches well with the region with low transmittance near $\Lambda=610$ nm.

Further, note that zero transmittance observed at $\Lambda<320$ nm arises from the grating equation. For thin diffraction gratings, the incident beam with an angle of θ_i is converted into several waves at angles θ_l satisfying

$$\sin\theta_l = \sin\theta_i + l\frac{\lambda}{\Lambda}, \tag{7}$$

where an integer l denotes the diffraction order. When a silver grating has a period $\Lambda<\lambda/2$, it is unachievable to obtain the first diffraction order out of propagating surface plasmons and thus, transmittance by the first-order diffraction is determined to be zero at $\Lambda<320$ nm. From the above interpretations, it should be emphasized that a careful design study is demanded to avoid the geometry-dependent absorption band, plasmon radiation damping, and zero transmittance.

In the case of the CE, Fig. 6(b) demonstrates the distributions of CE values and CE_{MAX} of 85.7% was obtained at $d_g=24$ nm and $\Lambda=320$ nm. The trends of reduced CE caused by various plasmonic effects resemble the results of the transmittance.

As an example of the actual application of the proposed transmission-type SPR configuration designed to provide a high diffraction efficiency, silver substrates based on a rectangular silver grating with $d_g=12$ nm and $\Lambda=330$ nm are now applied as a biosensor to detect biomolecular interactions occurring at a sensor surface. Compared with our earlier application of silver gratings to detect a change of gaseous and aqueous ambience [6], it is more appropriate to consider binding events in an aqueous solution because it is of practical importance in biochemical experiments. Target binding between biomolecules is modeled as 3-nm-thick dielectric monolayer whose refractive index changes from 1.33, i.e., no target analytes in water solutions, to 1.70 in accordance with the concentration of adsorbed analytes. Fig. 8 shows that, since the resonance angle is sensitive to the local change in the environment surrounding a metal film, the presence of silver gratings led to a larger resonance angle compared with a conventional SPR structure. Moreover, using the linear regression analyses with a function of $y=Ax+B$, the linear coefficient (A) and the correlation coefficient (R), where R denotes the degree of the linearity, are equal to 2.29 and 0.9976 for a conventional SPR scheme and 3.32 and 0.9993 for a transmission-type one. In other words, a silver grating can provide an enhanced sensitivity by more than 45%. This sensitivity improvement by RCWA calculations corresponds well with measured data obtained from biomolecular interactions [21]. While gold substituted for silver, sensitivity enhancement ranging from 24% to 57% was measured for layered biointeractions when rectangular gold gratings on a thin gold film have $\Lambda=300$ nm and $d_g=10$ nm. The plasmonic description based on a surface-limited increase of reaction area and strong excitation of LSP modes can be adopted to explain the enhanced sensitivity. Especially, localized and highly enhanced plasmons interact with biomolecular binding events close to metallic gratings and subsequently cause a larger shift of resonant LSP modes. The field enhancement has been investigated as an efficient way to enhance the sensitivity limit that has long plagued a conventional SPR biosensor [22,23].

In addition to sensitivity enhancement, a figure of merit (FOM) [24] is employed to effectively compare the overall sensor performance as

$$\mathrm{FOM} = \frac{m[\mathrm{deg/RIU}]}{\mathrm{CAW[deg]}}(1-\mathrm{MRR}). \tag{8}$$

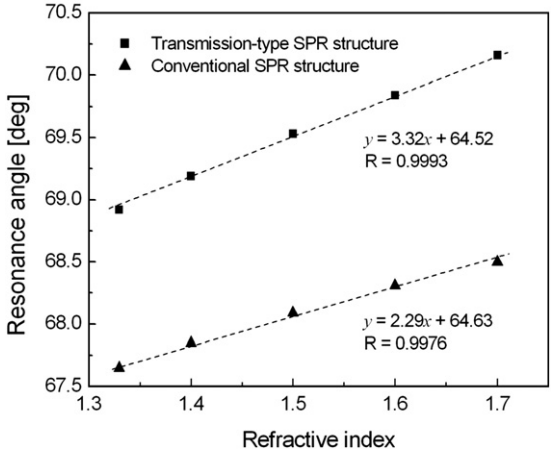

Fig. 8. Linear regression analyses between resonance angle and refractive index of a dielectric binding layer for an SPR biosensor with and without a silver grating at $d_g=12$ nm and $\Lambda=330$ nm in a water medium.

Here, m is the sensitivity, i.e., the slope of the resonance angle over the refractive index range, which corresponds to the linear coefficient A in linear regression analyses. RIU stands for refractive index unit. The curve angular width (CAW) and minimum reflectance at resonance (MRR) denote the full angular width at the center of reflectance minimum and maximum and the reflectance value at the point of SPR angle, respectively. Thus, a smaller CAW and a lower MRR are required because a narrower and deeper SPR curve allows an efficient detection of the resonance and precise examination of sensing events. From our numerical results, FOM values were determined to be 0.676 for a conventional SPR structure and 1.184 for a transmission-type one. As a result, a transmission-type SPR biosensor with rectangular silver gratings exhibits better sensing performance by more than 1.7 times in comparison with a SPR biosensor without silver gratings.

Fabrication work is also currently under way for demonstration. Rectangular silver gratings can be achieved by plasma etching that follows sputtering of silver layer and e-beam or interference lithography processes.

4. Conclusion

In this study, transmission-type SPR configuration with a silver grating has been investigated as a structure that can emit propagating surface plasmons efficiently. When $\lambda = 633$ nm and a fill factor is fixed at 0.5, rectangular silver gratings presented a notable performance in terms of transmittance and CE. From an in-depth study for a wide range of grating periods and thicknesses, silver gratings were found to provide a peak transmittance of 64.1% at $d_g = 12$ nm and $\Lambda = 330$ nm and a maximal CE value of 85.7% at $d_g = 24$ nm and $\Lambda = 320$ nm. In addition, an abrupt reduction in transmittance and CE was discussed based on various plasmon damping effects.

It was also found that the diffracted beam intensity can be decreased significantly with an increasing Ag_2O thickness. To overcome this limitation accompanied by silver substrates susceptible to oxidation, a silver grating combined with a thin gold layer was explored. Finally, as a practical sensing application, silver grating-mediated SPR structure in a water ambience showed a notable SPR signal amplification, which is associated with strong excitation of LSP modes and an increased surface reaction area. This study shows the potential of using transmitted SP waves in a variety of optical applications, such as optical imaging system, optical biosensor, and light sources.

Acknowledgments

This work was supported by Korea Science and Engineering Foundation (KOSEF) grant funded by the Korean government (MEST) (2009-0069267) and partially supported by the Korea Research Foundation grant funded by the Korean Government Basic Research Promotion Fund (MOEHRD)-(KRF-2008-331-D00229). The work of Sung June Kim was financially supported by the grant from the Industrial technology development program (10033657) of the Ministry of Knowledge Economy (MKE) of Korea and by Pioneer research program through the National Research Foundation of Korea funded by the Ministry of Education, Science and Technology (2010-0002249).

References

[1] E. Ozbay, Science 311 (2006) 189.
[2] H. Raether, Surface Plasmons on Smooth and Rough Surfaces and on Gratings, Springer Tracts in Modern Physics, Springer-Verlag, 1988.
[3] S. Park, G. Lee, S.H. Song, C.H. Oh, P.S. Kim, Opt. Lett. 28 (2003) 1870.
[4] C. Lenaerts, F. Michel, B. Tilkens, Y. Lion, Y. Renotte, Appl. Opt. 44 (2005) 6017.
[5] S.H. Choi, S.J. Kim, K.M. Byun, Appl. Opt. 48 (2009) 2924.
[6] K.M. Byun, S.J. Kim, D. Kim, Appl. Opt. 46 (2007) 5703.
[7] M.G. Moharam, T.K. Gaylord, J. Opt. Soc. Am. A 3 (1986) 1780.
[8] K.M. Byun, S.J. Yoon, D. Kim, S.J. Kim, Opt. Lett. 32 (2007) 1902.
[9] J. Cesario, R. Quidant, G. Badenes, S. Enoch, Opt. Lett. 30 (2005) 3404.
[10] Y. Kanamori, K. Hane, H. Sai, H. Yugami, Appl. Phys. (N.Y.) 78 (2001) 142.
[11] M.G. Moharam, T.K. Gaylord, J. Opt. Soc. Am. 73 (1983) 451.
[12] M.G. Moharam, T.K. Gaylord, J. Opt. Soc. Am. 72 (1982) 1385.
[13] L. Li, C.W. Haggans, J. Opt. Soc. Am. A 10 (1993) 1184.
[14] J. Homola, S.S. Yee, G. Gauglitz, Sens. Actuators B 54 (1999) 3.
[15] H. Libardi, H.P. Grieneisen, Thin Solid Films 333 (1998) 82.
[16] S.J. Yoon, D. Kim, J. Opt. Soc. Am. A 25 (2008) 725.
[17] M.F. Al-Kuhaili, J. Phys. D: Appl. Phys. 40 (2007) 2847.
[18] A.I. Stognij, N.N. Novitskii, S.D. Tushina, S.V. Kalinnikov, Tech. Phys. 48 (2003) 745.
[19] J.P. Kottmann, O.J.F. Martin, D.R. Smith, S. Schultz, Phys. Rev. B 64 (2001) 235402.
[20] G. Schider, J.R. Krenn, W. Gotschy, B. Lamprecht, H. Ditlbacher, A. Leitner, F.R. Aussenegg, J. Appl. Phys. 90 (2001) 3825.
[21] K. Kim, D.J. Kim, S. Moon, D. Kim, K.M. Byun, Nanotechnology 20 (2009) 315501.
[22] T. Okamoto, I. Yamaguchi, T. Kobayashi, Opt. Lett. 25 (2000) 372.
[23] E. Hutter, J.H. Fendler, Adv. Mater. 16 (2004) 1685.
[24] L.J. Sherry, S.-H. Chang, G.C. Schatz, R.P. Van Duyne, B.J. Wiley, Y. Xia, Nano Lett. 5 (2005) 2034.